



Cite this: *Chem. Commun.*, 2019, 55, 14906

Received 28th October 2019,  
Accepted 15th November 2019

DOI: 10.1039/c9cc08423a

rsc.li/chemcomm

We report the synthesis and self-assembly behavior of a chiral  $C_3$ -symmetrical benzene-tricarboxylic selenoamide. The introduction of the selenoamide moiety enhances the dipolar character of the supramolecular interaction and confers a remarkable thermal stability to the supramolecular polymers obtained.

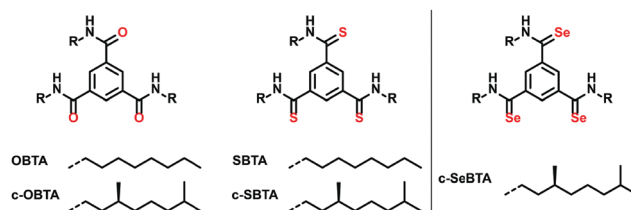
Supramolecular chemistry has matured up to a point where parallelisms between sophisticated multi-step covalent syntheses and the construction of increasingly complex, artificial supramolecular systems become more and more apparent.<sup>1–4</sup> Recent developments in living supramolecular polymerizations,<sup>5–8</sup> controlled supramolecular copolymerizations<sup>9–12</sup> and the design of unconventional thermal behaviour in supramolecular polymers<sup>13–15</sup> resulted in unprecedented control in length and microstructure of the formed polymers. Like in proteins, one of the central interactions underlying the stability and structure of many supramolecular systems is the formation of hydrogen bonds between amides. This ubiquitous interaction comprises several contributions such as dispersion interactions, electrostatics, polarization and charge transfer.<sup>16</sup> Recently, it has become evident that the replacement of oxygen in amide bonds by other chalcogens such as sulphur and selenium retains the ability of the resulting thio- and selenoamides to engage in hydrogen bonding interactions.<sup>17–20</sup> In addition, it has been observed both theoretically and experimentally that  $\text{NH}\cdots\text{S}$  or  $\text{NH}\cdots\text{Se}$  hydrogen bonds can be as strong as those of  $\text{NH}\cdots\text{O}$ , despite the lower electronegativity of S and Se.<sup>21,22</sup> In proteins

and peptides, the introduction of thioamide or selenoamide bonds has allowed to tune their structure, stability, and – in case of enzymes – activity.<sup>23–26</sup> Interestingly, as the chalcogen atom in the amide in peptides changes from O to S to Se, the increasing polarizability was found to increasingly dominate the electronic properties of the amides. As a result, the amide structure becomes increasingly characterized by the resonance form with negative charge on S or Se upon going down the periodic table.<sup>27</sup> While the replacement of oxygen with sulphur typically results in a larger effect, the consequence of the further S to Se substitution is more modest, yet still detectable. As charge separation and dipolar interactions have been linked to cooperative behaviour in supramolecular polymers,<sup>28</sup> selenoamides may provide interesting functionality in these non-covalent structures.

In the past we have extensively investigated the self-assembly of  $C_3$ -symmetrical  $N,N',N''$ -trialkylbenzene-1,3,5-tricarboxamides (**OBTAs**) in apolar alkane solvents (achiral **OBTA** and chiral **c-OBTA**, Scheme 1) and more recently also of  $N,N',N''$ -trialkylbenzene-1,3,5-trithioamides (**SBTAs**) (achiral **SBTA** and **c-SBTA**, Scheme 1).<sup>29,30</sup>

Stimulated by the increased dipolar character of the interactions between thioamides as compared to normal amides,<sup>31–33</sup> we hypothesized that moving one row further down the periodic

### Previous work This work



Scheme 1 Chemical structures of previously reported **OBTA**, **c-OBTA**, **SBTA** and **c-SBTA**; chemical structure of the chiral selenoamide derivative **c-SeBTA** introduced in this work. Enantiopure compounds are indicated with the prefix **c-**.

<sup>a</sup> Institute for Complex Molecular Systems, Eindhoven University of Technology, P. O Box 513, 5600 MB Eindhoven, The Netherlands. E-mail: a.palmans@tue.nl, e.w.meijer@tue.nl

<sup>b</sup> Department of Organic Chemistry, Universidad Autónoma de Madrid (UAM), Calle Francisco Tomás y Valiente, 7, 28049 Madrid, Spain

<sup>c</sup> IMDEA Nanociencia, c/Faraday 9, Cantoblanco, Spain

† Electronic supplementary information (ESI) available: Experimental details, synthesis and characterization of all new compounds, spectroscopic details, modeling details, temperature- and solvent-dependent supramolecular polymerization studies and fits. See DOI: 10.1039/c9cc08423a

‡ These authors have contributed equally.



table to selenoamides would affect the stability of the formed cooperative supramolecular polymers. In addition, we anticipated that in copolymerizations the microstructure of the copolymers could be modulated.

Here, we disclose the synthesis (reported in the ESI<sup>†</sup>) and self-assembly of the chiral,  $C_3$ -symmetrical benzene-tricarboxylic selenoamide **c-SeBTA** (Scheme 1). We compare its self-assembly behavior to that of **OBTA/c-OBTA**<sup>20</sup> and **SBTA/c-SBTA**.<sup>21</sup> The different nature of the selenoamide hydrogen bond is illustrated by our finding that **c-SeBTA** polymers have an increased stability towards thermal denaturation yet enhanced lability towards polar solvents-induced denaturation.

The chiral tricarboxylic selenoamide **c-SeBTA** was synthesized in 82% yield by refluxing **c-OBTA** with Woollins reagent ( $\text{Ph}_2\text{P}_2\text{Se}_4$ ) in toluene (Scheme S1, ESI<sup>†</sup>).<sup>34</sup> We monitored the successful conversion to selenoamides by Fourier-transform infrared (FT-IR) spectroscopy. The disappearance of the parent carboxamide  $\text{C}=\text{O}$  vibration at  $1634\text{ cm}^{-1}$  was coupled to the appearance of a new vibration centered at  $1538\text{ cm}^{-1}$ , indicative for the formation of the desired product (Fig. S3–S5, ESI<sup>†</sup>). The N–H stretching vibration also shifted from  $3220\text{ cm}^{-1}$  to  $3151\text{ cm}^{-1}$  in the **c-OBTA** to **c-SeBTA** conversion. Further details on the molecular characterization of **c-SeBTA** can be found in the ESI<sup>†</sup>.

Chiral **SeBTA** was obtained as a yellow solid. The yellow color remained upon storing the compound under argon. However, exposing the samples to air for several hours resulted in an irreversible color change (Fig. S6, ESI<sup>†</sup>), suggesting decomposition. The low air stability of **c-SeBTA** was also coupled to poor thermal stability in ambient atmospheres, as we could not detect any transition upon heating or cooling due to decomposition of the samples by differential scanning calorimetry (DSC). Traces of **c-OBTA** detected in mass spectrometry suggest that **c-SeBTA** can react with moisture to form **c-OBTA** and other degradation products. Hence, the conversion of the tricarboxamides into triselenoamides implies particular attention concerning the compound's storage and preservation (under argon and preferably refrigerated).

We first studied the self-assembly behavior of **c-SeBTA** in apolar alkane solvents with ultraviolet-visible (UV-Vis) and circular dichroism (CD) spectroscopy. Upon dissolution of **c-SeBTA** in methylcyclohexane (MCH) at  $50\text{ }\mu\text{M}$  and thorough degassing, an absorption maximum at  $342\text{ nm}$  was observed in the UV-vis spectrum (Fig. 1a, bottom part). This maximum was red-shifted with respect to the spectrum of **c-SeBTA** in methanol (Fig. 1a, bottom part), suggesting self-assembly in the alkane solvent. In addition, a bisignate CD spectrum was obtained in MCH (maxima/minima at  $357\text{ nm}$ ,  $297\text{ nm}$  and  $252\text{ nm}$ ), which corroborated the presence of aggregates characterized by a preferred helical sense (Fig. 1a, top part). AFM measurements confirmed that aggregates of **c-SeBTA** are one-dimensional supramolecular polymers (Fig. S7, ESI<sup>†</sup>).

We employed variable temperature CD (VT-CD) spectroscopy to investigate the stability of the supramolecular polymers of **c-SeBTA**. We followed the intensity of the CD band centered at  $357\text{ nm}$  (Fig. 1b). Careful degassing of the prepared solutions was pivotal to ensure the reproducibility of the experiments

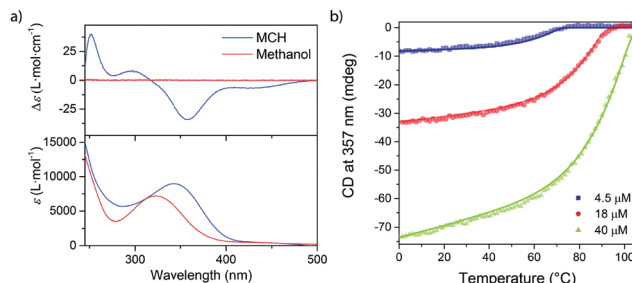


Fig. 1 (a) CD (top) and UV-vis (bottom) spectra of  $50\text{ }\mu\text{M}$  solutions of **c-SeBTA** in MCH and methanol (blue and red trace, respectively). (b) Variable temperature CD spectroscopy of solutions of **c-SeBTA** in MCH. Symbols indicate data and the solid lines indicate the global fit.

(for the degassing procedure see ESI<sup>†</sup>). The  $40\text{ }\mu\text{M}$  solutions of **c-SeBTA** showed CD activity up to temperatures as high as  $100\text{ }^\circ\text{C}$ , indicating the high thermal stability of the generated supramolecular polymers (Fig. 1b, green trace). Upon decreasing the concentration to  $18\text{ }\mu\text{M}$  (Fig. 1b, red trace) and  $4.5\text{ }\mu\text{M}$  (Fig. 1b, blue trace), a sharp transition between the CD-silent monomerically dissolved **c-SeBTA** to the supramolecular polymers of **c-SeBTA** was observed at  $93\text{ }^\circ\text{C}$  and  $75\text{ }^\circ\text{C}$ , respectively. This indicated a polymerization process characterized by a cooperative mechanism. By fitting the experimental data to a nucleation–elongation model,<sup>35</sup> we determined enthalpy ( $\Delta H_e$ ) and entropy ( $\Delta S_e$ ) of elongation equal to  $-75\text{ kJ mole}^{-1}$  and  $-97\text{ J mole}^{-1}\text{ K}^{-1}$ , respectively, and a nucleation penalty of  $21\text{ kJ mole}^{-1}$ . The latter corresponds to a cooperativity factor,  $\sigma$ , of  $2 \times 10^{-4}$  at  $293\text{ K}$ . Compared to the supramolecular polymers of **c-SBTA** ( $\Delta H_e = -65.7\text{ kJ mole}^{-1}$ ),<sup>30,36</sup> the enthalpic contribution in the supramolecular polymerization of **c-SeBTA** was slightly more favorable, suggesting stronger intermolecular interactions in the case of the selenoamides. The entropic penalty of the supramolecular polymerization of **c-SeBTA** ( $\Delta S_e = -97\text{ J mole}^{-1}\text{ K}^{-1}$ ) was comparable to that of **c-SBTA**<sup>30,36</sup> ( $\Delta S_e = -102.6\text{ J mole}^{-1}\text{ K}^{-1}$ ), instead, and we speculate similar ordering between the homopolymers of **c-SeBTA** and **c-SBTA**. We rationalize these thermodynamic parameters with an increased dipole–dipole and charge transfer character of the diffuse Se–NH hydrogen bond,<sup>21,37</sup> which ultimately affords the increased thermal stability of the supramolecular polymers of **c-SeBTA** (more favorable  $\Delta H_e$  and very similar  $\Delta S_e$  compared to **c-SBTA**). Interestingly, the nucleation penalty, and hence cooperativity, of the supramolecular polymers of **c-SBTA** and **c-SeBTA** were comparable ( $\sigma = 1.9 \times 10^{-3}$  for **c-SBTA**,<sup>30,36</sup> and  $3 \times 10^{-4}$  for **c-SeBTA**). This is in strong contrast to the lower cooperativity of **c-SBTA** compared to **c-OBTA** ( $\sigma < 10^{-6}$ ).<sup>30,36</sup>

Next to VT-CD spectroscopy, the supramolecular polymerization of **c-SeBTA** was also investigated by changing the solvent quality in a denaturation experiment. Analogously to a previous study on **c-SBTA**<sup>38</sup> discrete aliquots of  $\text{CHCl}_3$  (good solvent) were added to  $20\text{ }\mu\text{M}$  solutions of **c-SeBTA** in MCH and the intensity of the CD signal was monitored (Fig. 2a and b). Upon increasing the solvent quality by adding  $\text{CHCl}_3$ , the CD effect decreased in intensity (Fig. 2a). Above 4 vol%, no CD intensity could be observed anymore, indicating the complete destabilization of the polymers in 96 : 4 MCH :  $\text{CHCl}_3$  (Fig. 2a). When monitoring the



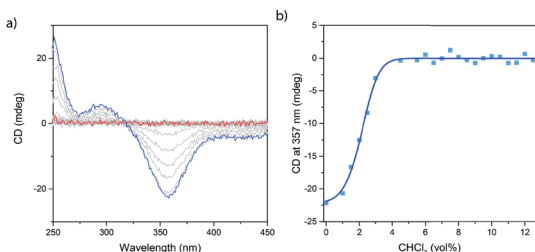


Fig. 2 Denaturation experiment of **c-SeBTA**. (a) Change of the CD spectra of **c-SeBTA** (20  $\mu$ M in MCH, blue line) upon adding CHCl<sub>3</sub> (0–12 vol%, red line) and (b) CD effect at 357 nm as a function of the amount of CHCl<sub>3</sub>. The squares indicate experimental data and the solid lines represent the simulation.

maximum CD intensity at 357 nm, a clear non-sigmoidal dependency on the solvent quality is obtained (Fig. 2b), confirming the cooperative polymerization mechanism observed in the VT-CD experiments. The critical solvent fraction of 4 vol% CHCl<sub>3</sub> in MCH at 20  $\mu$ M for **c-SeBTA** is in remarkable contrast with a critical CHCl<sub>3</sub> fraction of 20 vol% obtained for **c-SBTA**.<sup>38</sup> This was unexpected, given the similar thermal behavior of the supramolecular polymers of **c-SeBTA** and **c-SBTA** discussed above. To obtain more insights into the thermodynamic properties of the denaturation process, the spectroscopic data were fitted to a mass-balance model that describes the destabilization of supramolecular polymers.<sup>38</sup> For **c-SeBTA**, we obtain a Gibbs free energy of elongation ( $\Delta G_e^{\text{den}}$ ) of  $-36 \text{ kJ mole}^{-1}$  in MCH, a solvent dependency parameter ( $m$ ) of  $602 \text{ kJ mole}^{-1}$ , as well as a nucleation penalty of  $2.6 \text{ kJ mole}^{-1}$ . This Gibbs free energy of elongation is comparable to the Gibbs free energy of  $-40 \text{ kJ mole}^{-1}$  reported for **c-SBTA**, but the solvent dependency parameter,  $m$ , obtained for **c-SeBTA** is six fold higher than the  $103 \text{ kJ mole}^{-1}$  reported for **c-SBTA**.<sup>38</sup> We conclude that the enhanced charge separation in selenoamides<sup>27</sup> increases the solubility in the relatively polar CHCl<sub>3</sub> solvent. As a result, the interaction of the monomer with the polar co-solvent is enhanced and smaller amounts of co-solvent are needed to completely denature the polymer. Thus, on one side installing the selenoamide motif increases the thermal stability of the resulting supramolecular polymers in pure alkane solvents, while it simultaneously decreases their stability in more polar environments.

Besides influencing the stabilities of the supramolecular homopolymers, the different polarizability of oxygen, sulfur and selenium offers attractive possibilities to tune the interactions between monomers in supramolecular copolymers. We carried out mixed sergeants and soldiers experiment using **c-SeBTA** as sergeant for **OBTA** and **SBTA** to investigate the interaction between these supramolecular monomers (Fig. 3). The gradual titration of chiral **c-SeBTA** to a 30  $\mu$ M solution of achiral **OBTA** in MCH resulted in the appearance of a CD spectrum typically observed for **c-OBTA** (Fig. S9a, ESI†), indicating that **OBTA** and **c-SeBTA** form copolymers. Complete chiral amplification was obtained by adding more than 30 mol% of **c-SeBTA**, as suggested by the saturation of the CD signal with respect to the intensity expected for a 30  $\mu$ M solution of **c-OBTA** (Fig. 3 top panel). Analogously, addition of **c-SeBTA** to a 30  $\mu$ M solution of **SBTA** resulted in the appearance of a CD spectrum

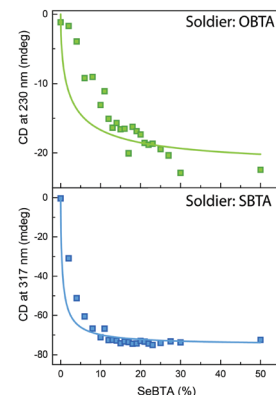


Fig. 3 Sergeants and soldiers experiment of **c-SeBTA** sergeants with 30 mol% **OBTA** soldiers (top panel) and **SBTA** soldiers (bottom panel) in MCH. The squares indicate experimental data and the solid lines represent the simulation.

typically observed for **c-SBTA**,<sup>36</sup> which indicated successful copolymerization (Fig. S9b, ESI†). **c-SeBTA** was more effective in biasing the helical sense in the case of **SBTA**: only 12 mol% **c-SeBTA** was required to achieve full chiral amplification (Fig. 3 bottom panel). We applied the model developed by Markvoort and ten Eikelder<sup>10,39</sup> to quantify the heterointeraction of **c-SeBTA** with **OBTA** and **SBTA** in the sergeants and soldiers experiment. These heterointeractions are dependent on the two homopolymerizations through an  $\alpha$ -parameter (eqn (1)),<sup>30</sup>

$$\Delta G_{\text{hetero}} = \frac{1}{2} \cdot \alpha \cdot (\Delta G_{e,\text{SeBTA}} + \Delta G_{e,\text{XBTA}}) \quad (1)$$

with  $\Delta G_{\text{hetero}}$  the Gibbs free energy of the interaction between **c-SeBTA** and **OBTA** or **SBTA**,  $\Delta G_{e,\text{SeBTA}}$  the Gibbs free energy of the elongation of the **c-SeBTA** homopolymer, and  $\Delta G_{e,\text{XBTA}}$  the Gibbs free energy of the elongation of the **OBTA** or **SBTA** homopolymer.

The thermodynamic values for **OBTA** and **SBTA** have been described elsewhere.<sup>30</sup> We obtained a good agreement between our experimental results and the model prediction for **SBTA/c-SeBTA** when using  $\alpha = 0.815$  (Fig. 3 bottom panel and Table 1). This value is lower than that previously reported for the nearly random copolymers of **SBTA/OBTA** ( $\alpha = 0.92$ )<sup>29</sup> but higher than those of the blocky copolymers formed by triarylamine-based systems ( $\alpha = 0.57$ ).<sup>10</sup> This indicates that the copolymers of **c-SeBTA/SBTA** have a slightly blocky microstructure. In contrast, we could not find a good agreement between the model and the experimental data of **OBTA/c-SeBTA** (best fit for  $\alpha = 0.72$ , Fig. 3 top panel). Most likely, the assumption made in the model that  $\Delta G_{\text{hetero}}$  is identical for  $\text{O}=\text{CNH}\cdots\text{Se}=\text{C}$  and  $\text{Se}=\text{CNH}\cdots\text{O}=\text{C}$

Table 1 Thermodynamic values (20 °C) showing good agreement between model predictions and experimental results with **c-SeBTA** sergeants and **OBTA/SBTA** soldiers

	OBTA	SBTA
$\Delta G_{e,\text{XBTA}}$ (kJ mole <sup>-1</sup> )	-33.6	-36.4
$\alpha$	0.72	0.815
$\Delta G_{\text{hetero}}$ (kJ mole <sup>-1</sup> )	-28.9	-33.8

does not hold. The energetic difference between the XBTA homopolymerization ( $X = O$  or  $S$ ) and the heterointeraction was smaller for the **c-SeBTA/SBTA** couple compared to the **c-SeBTA/OBTA** one (Table 1). The smaller difference in interaction strength for the neighboring chalcogens suggests that it is the polarizability of the groups that governs the interaction strength between the different monomers in the copolymerization. Hence, tuning heterointeractions by means of polarizability of the interacting co-monomers may prove to be an attractive way to tune supramolecular copolymerizations and control the microstructure of the resulting copolymers.

In conclusion, similarly to their oxygen and sulfur analogues, selenoamide-based discotic molecules self-assemble through hydrogen bond formation in apolar alkane solvents. The introduction of the selenoamides further increases the dipole–dipole and charge transfer interactions in the hydrogen bonding and continues a trend which was already observed upon changing carboxamides to thioamides.<sup>36</sup> As a result, **c-SeBTA** shows an enhanced stability towards thermal denaturation in apolar alkane solvents while also showing an increased sensitivity towards polar co-solvents. Additionally, the subtle role played by polarizability and dipole–dipole interactions in hydrogen bonds offers an attractive way to design and control supramolecular copolymers. We showed successful copolymerization of **c-SeBTA** with **OBTA** and **SBTA** through sergeants and soldiers experiments. The interaction strength is highest for neighboring chalcogens, leading to the possibility to tune the supramolecular copolymerization through modulation of the dipole–dipole and charge transfer interactions in hydrogen bonds. We propose that our results will allow further control in the design of novel supramolecular polymers and serve as inspiration for further theoretical and experimental investigations into selenoamide hydrogen bonds.

Lafayette de Windt is gratefully acknowledged for providing the achiral **OBTA** and **SBTA** and for fruitful discussions. Tristan Mes and Elisa Huerta are acknowledged for the initial experiments. The authors thank NWO for financial support.

## Conflicts of interest

There are no conflicts to declare.

## Notes and references

1. N. Giuseppone, *Acc. Chem. Res.*, 2012, **45**, 2178–2188.
2. J. Lehn, *Angew. Chem., Int. Ed.*, 2013, **52**, 2836–2850.
3. P. Besenius, *J. Polym. Sci., Part A: Polym. Chem.*, 2017, **55**, 34–78.
4. G. Vantomme and E. W. Meijer, *Science*, 2019, **363**, 1396–1397.
5. S. Ogi, K. Sugiyasu, S. Manna, S. Samitsu and M. Takeuchi, *Nat. Chem.*, 2014, **6**, 188–195.
6. T. Fukui, S. Kawai, S. Fujinuma, Y. Matsushita, T. Yasuda, T. Sakurai, S. Seki, M. Takeuchi and K. Sugiyasu, *Nat. Chem.*, 2017, **9**, 493–499.
7. W. Wagner, M. Wehner, V. Stepanenko, S. Ogi and F. Würthner, *Angew. Chem., Int. Ed.*, 2017, **56**, 16008–16012.

8. J. S. Valera, R. Gómez and L. Sánchez, *Small*, 2018, **14**, 1702437.
9. A. Pal, M. Malakoutikhah, G. Leonetti, M. Tezcan, M. Colomb-Delsuc, V. D. Nguyen, J. Van Der Gucht and S. Otto, *Angew. Chem., Int. Ed.*, 2015, **54**, 7852–7856.
10. B. Adelizzi, A. Alois, A. J. Markvoort, H. M. M. ten Eikelder, I. K. Voets, A. R. A. Palmans and E. W. Meijer, *J. Am. Chem. Soc.*, 2018, **140**, 7168–7175.
11. S. H. Jung, D. Bochicchio, G. M. Pavan, M. Takeuchi and K. Sugiyasu, *J. Am. Chem. Soc.*, 2018, **140**, 10570–10577.
12. S. Chakraborty, D. Ray, V. K. Aswal and S. Ghosh, *Chem. – Eur. J.*, 2018, **24**, 16379–16387.
13. T. Vermonden, J. Van Der Gucht, P. De Waard, A. T. M. Marcelis, N. A. M. Besseling, E. J. R. Sudhölter, G. J. Fleer and M. A. Cohen Stuart, *Macromolecules*, 2003, **36**, 7035–7044.
14. K. Venkata Rao, D. Miyajima, A. Nihonyanagi and T. Aida, *Nat. Chem.*, 2017, **9**, 1133–1139.
15. V. Grande, B. Soberats, S. Herbst, V. Stepanenko and F. Würthner, *Chem. Sci.*, 2018, **9**, 6904–6911.
16. T. Steiner, *Angew. Chem., Int. Ed.*, 2002, **41**, 48–76.
17. C. Alemán, *J. Phys. Chem. A*, 2001, **105**, 6717–6723.
18. H.-J. Lee, Y.-S. Choi, K.-B. Lee, J. Park and C.-J. Yoon, *J. Phys. Chem. A*, 2002, **106**, 7010–7017.
19. D. Bibelaiy, A. S. Lundemba, F. H. Allen, P. T. A. Galek, J. Pradon, A. M. Reilly, C. R. Groom and Z. G. Yav, *Acta Crystallogr., Sect. B: Struct. Sci., Cryst. Eng. Mater.*, 2016, **72**, 317–325.
20. V. R. Mundlapati, S. Gautam, D. K. Sahoo, A. Ghosh and H. S. Biswal, *J. Phys. Chem. Lett.*, 2017, **8**, 4573–4579.
21. K. K. Mishra, S. K. Singh, P. Ghosh, D. Ghosh and A. Das, *Phys. Chem. Chem. Phys.*, 2017, **19**, 24179–24187.
22. V. R. Mundlapati, D. K. Sahoo, S. Ghosh, U. K. Purame, S. Pandey, R. Acharya, N. Pal, P. Tiwari and H. S. Biswal, *J. Phys. Chem. Lett.*, 2017, **8**, 794–800.
23. T. T. Tran, J. Zeng, H. Treutlein and A. W. Burgess, *J. Am. Chem. Soc.*, 2002, **124**, 5222–5230.
24. D. Wildemann, C. Schiene-Fischer, T. Aumüller, A. Bachmann, T. Kieflhaber, C. Lücke and G. Fischer, *J. Am. Chem. Soc.*, 2007, **129**, 4910–4918.
25. Y. Huang, G. Jahreis, C. Lücke, D. Wildemann and G. Fischer, *J. Am. Chem. Soc.*, 2010, **132**, 7578–7579.
26. C. R. Walters, D. M. Szantai-Kis, Y. Zhang, Z. E. Reinert, W. S. Horne, D. M. Chenoweth and E. J. Petersson, *Chem. Sci.*, 2017, **8**, 2868–2877.
27. Y. Huang, G. Jahreis, G. Fischer and C. Lücke, *Chem. – Eur. J.*, 2012, **18**, 9841–9848.
28. C. Kulkarni, S. Balasubramanian and S. J. George, *ChemPhysChem*, 2013, **14**, 661–673.
29. M. M. J. Smulders, A. P. H. J. Schenning and E. W. Meijer, *J. Am. Chem. Soc.*, 2008, **130**, 606–611.
30. L. N. J. de Windt, C. Kulkarni, H. M. M. ten Eikelder, A. J. Markvoort, E. W. Meijer and A. R. A. Palmans, *Macromolecules*, 2019, **52**, 7430–7438.
31. O. Exner and K. Waisser, *Collect. Czech. Chem. Commun.*, 1982, **47**, 828–837.
32. K. B. Wiberg and P. R. Rablen, *J. Am. Chem. Soc.*, 1995, **117**, 2201–2209.
33. K. B. Wiberg and D. J. Rush, *J. Am. Chem. Soc.*, 2001, **123**, 2038–2046.
34. P. Bhattacharyya and J. D. Woollins, *Tetrahedron Lett.*, 2001, **42**, 5949–5951.
35. D. Zhao and J. S. Moore, *Org. Biomol. Chem.*, 2003, **1**, 3471–3491.
36. T. Mes, S. Cantekin, D. W. R. Balkenende, M. M. M. Frissen, M. A. J. Gillissen, B. F. M. De Waal, I. K. Voets, E. W. Meijer and A. R. A. Palmans, *Chem. – Eur. J.*, 2013, **19**, 8642–8649.
37. A. Kjaersgaard, J. R. Lane and H. G. Kjaergaard, *J. Phys. Chem. A*, 2019, **123**, 8427–8434.
38. P. A. Korevaar, C. Schaefer, T. F. A. De Greef and E. W. Meijer, *J. Am. Chem. Soc.*, 2012, **134**, 13482–13491.
39. H. M. M. ten Eikelder, B. Adelizzi, A. R. A. Palmans and A. J. Markvoort, *J. Phys. Chem. B*, 2019, **123**, 6627–6642.

